Ecological Modelling 291 (2014) 218–223

Contents lists available at ScienceDirect

Ecological Modelling

journal homepage: www.elsevier.com/locate/ecolmodel

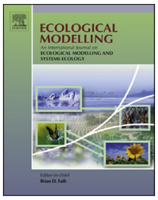

Modelling Late Pleistocene megafaunal extinction and critical cases: A simple prey–predator perspective

J.C. Flores*

Instituto de Alta Investigación IAI, Universidad de Tarapacá, Casilla 7-D, Arica, Chile

ARTICLE INFO

Article history:
Received 22 May 2014
Received in revised form 1 August 2014
Accepted 5 August 2014
Available online 29 August 2014

Keywords:
Population dynamics
Coupled nonlinear
Prey–predator
Megafauna extinction

ABSTRACT

Using a nonlinear prey–predator model, we establish the extinction threshold for megafauna in the Late Pleistocene and predict extinction times since the arrival of hunters. The threshold is related to growth and depredation rates. From archaeological data, ecological findings, and the overkill hypothesis, the elapsed extinction times in Australia and North America are roughly estimated as 4800 and 3000 years, respectively. In Africa, the extinction times follow a particular power-law behavior with a critical time of the order of 185,000 years, roughly corresponding to the emergence of anatomically modern humans. Most of the parameters are estimated from a living representative megafauna prototype; the African elephant (*Loxodonta africana*). The elapsed time becomes a function of the effective area and the human diffusion coefficient. From allometric considerations, we can understand why small species were not decimated by depredation in the Late Pleistocene.

1. Introduction

The extinction of terrestrial megafauna in the Late Pleistocene (approximately 120,000–15,000 years before present (BP)) was not localized to particular habitats, and its primary cause remains controversial (Koch, 2006; Foster, 2003). As is well-documented, giant vertebrates existed in many ecosystems, and extinctions were important events that triggered ecological transformations. Particularly, extinction in the Late Pleistocene is thought to be related to either external environmental changes or human arrivals. Evidence exists that humans used intentional fire as a type of prehistoric weapon of mass destruction (Daniau et al., 2010). The present article supports the idea that control and extensive use of fire by anatomically modern humans was a determinant behavioral innovation that assisted global spread of the species (McBrearty and Brooks, 2000; Brown, 2009).

More explicitly, Rule (2012) suggested that megafaunal extinction in Australia some 50,000–45,000 years ago was governed by human arrival rather than by climatic changes. In the broad context of quaternary megafaunal extinction, Hortola and Martinez-Navarro (2013) claimed that humans decimated Neanderthal populations. It appears that anatomically modern humans directly intervened on the megafaunal niche by extended fire landscape and depredation.

This article assumes a relationship between the Late Pleistocene extinction and large-scale disruption by hunter activity. Nevertheless, human intervention and climatic changes are intermingled and both can explain megafaunal extinction in a multifaceted way (see for instance Gibbons, 2004). Indeed, by varying the parameters in our model, we could eventually introduce climatological effects such as reduction in growth rate caused by natural cycle dysfunction. Explicitly, by example, Kiltie (1984) studied seasonality fluctuations in the post-glacial period and reproductive rates of species with long gestation times. Troyer et al. (2014) studied relationships between growth rates and climatic variations for particular mammals, also, avian variation rates were considered by Saether and Bakke (2000). Mathematically similar topics have been covered in a variety of interesting studies (Mosimann and Martin, 1975; Martin, 1984; Whittington and Dyke, 1984; Belovsky, 1988; Mithen, 1993; Alroy, 2001). However, our analysis focuses on relating global-scale extinction times to territorial areas and human diffusion coefficients. Similar to our work, Hamilton and Buchanan (2007) considered a diffusion coefficient for modeling ancient people migrations. The concepts of metapopulation, extinction and colonization were studied by Elmhagen and Angerbjörn (2001). Other researchers have applied agent-based techniques to large scale human dispersal including Neanderthal dispersal (Callegari, 2013). Montoya et al. (2010) studied habitat fragmentation and eventual species extinctions, and proposed a threshold hypothesis.

---

* Tel.: +56 58 230334.
E-mail addresses: cflores@uta.cl, cflores.iai@gmail.com

http://dx.doi.org/10.1016/j.ecolmodel.2014.08.004
0304-3800/

Using algebraic relationships Charnov and Zuo (2011) quantified an extinction threshold related to the hunting–fishing rate and the adult mortality rate (this last expressed also as an allometric function of the adult mass). In our case, the extinction threshold becomes from dynamic nonlinear prey–predator equations (Sections 2 and 4).

Employing standard modeling tools of mathematical population dynamics, we analyzed a set of coupled differential equations describing a predator–prey model of human hunting and megafauna depredation at the end of the Pleistocene. We consider the stability and the extinction times of species decimated by the invaders. The condition for decimation (or ultimate coexistence) is explicitly investigated. The elapsed extinction time in the corresponding habitat emerges as straightforward function of the human diffusion parameter and the effective area.

The paper is structured as follows. The nonlinear model is proposed in Section 2 and its equilibrium points are revealed in Sections 3 and 4. The proposed extinction threshold (Section 4) is generic and applicable to a wide variety of cases. In Section 5 the overkill condition is mathematically formulated and used in the parameter estimation. In Section 6 the more relevant model parameters, including the elapsed extinction time, are roughly evaluated in three cases of megafaunal extinction (or threat): (a) Australia, (b) North America and (c) Africa critical case. Section 7 is devoted to allometric considerations – in particular, a conceptual mass threshold for extinction. Conclusions and remaining questions are presented in Section 8.

Finally, we note that different species were threatened in the large-scale terrestrial megafaunal extinction process (Koch, 2006). In fact, some of these species still exist (Section 7) and our deterministic model refers only to averaged numbers. Thus, we present a type of mean field theory (Le Bellac, 1992).

2. Proposed model

In this work we shall consider a generalized Leslie's predator–prey model (Leslie, 1948; Boccara, 2010) for two interacting groups, the megafauna M and modern humans H. Designing by t the variable time, the proposed coupled equations are given by

$$\frac{dM}{dt} = rM\left(1 - \frac{M}{K_M D(H)} - \frac{\delta}{rK_H}H\right), \tag{1}$$

$$\frac{dH}{dt} = r'H\left(1 - \frac{H}{K_H G(M)}\right) \tag{2}$$

where r and r' are the respective growth rates and the variables M and H represent the number of megafaunal and human individuals, respectively. The parameter δ represents the human depredation rate, which is usually difficult to estimate and depends on many factors, such as the (lithic) specialized technology, hunter strategies (fire management, group strategy), and prey defensive strategies. Moreover, as conjectured in the allometric discussion in Section 7, δ also depends on the body mass of the species. For simplicity, we assume a parameter that does not discriminate by age. The quantities K_M and K_H are the natural carrying capacities of megafauna and humans respectively, which largely depend for instance on climatological conditions. The functions $D(H)$ and $G(M)$ decrease and increase the carrying capacity, respectively, and account for carrying capacity perturbations on the niches. Both positive functions are assumed analytic and single-valued.

The model described by Eqs. (1) and (2) reduces to Leslie's model when $D(H)=$ constant and $G(M) \propto M$. Such a model has been widely applied in biological population dynamics, including a generalization to Allee effect (Gonzales, 2011; Murray, 2004) in ecology, understanding the Easter Island habitat collapse (Bologna and Flores, 2008) and others (Boccara, 2010).

Note that Eqs. (1) and (2) permit two routes of intervention by modern humans on the megafaunal population: (i) direct depredation via the one-by-one interaction term δ and (ii) indirect perturbation on the niche via the decreasing function $D(H)$. On the other hand, the carrying human perturbation factor $G(M)$ is related to human expansion subsequent to megafaunal habitat usurpation. Consequently, we impose the following conditions on the first derivatives:

$$\frac{dD}{dH} \le 0, \quad \text{and} \quad 0 \le \frac{dG}{dM}, \quad (D(0) = G(0) = 1). \tag{3}$$

The resulting inequalities

$$D(H) \le 1, \quad \text{and} \quad G(M) \ge 1, \tag{4}$$

will prove useful when determining the general properties of Eqs. (1) and (2). Finally, we emphasize that inequalities (4) are sufficient for our study goals, and that further specifications on D and G are not required.

3. Megafauna and human equilibrium points on axes

This section focuses on the three equilibrium points of Eqs. (1) and (2), which occur on the axes $(H=0, M)$ and $(H, M=0)$. The stability criteria are established by usual linearization techniques around these fixed points (Boccara, 2010; Murray, 2004; Lakshmanan and Rajasekar, 2002, see Appendices A and B for brief details).

(a) The first equilibrium point corresponds to the nonexistence of species M; mathematically, $M=0$ and $H=K_H$. Assuming $M=\eta$ and $H=K_H+\varepsilon$, with $\eta, \varepsilon \ll 1$, from Eqs. (1) and (2) the differential equation in the stability analysis is given by

$$\frac{d}{dt}\begin{pmatrix}\eta \\ \varepsilon\end{pmatrix} = \begin{pmatrix} r-\delta & 0 \\ r'K_H G'(0) & -r'\end{pmatrix}\begin{pmatrix}\eta \\ \varepsilon\end{pmatrix}. \tag{5}$$

The eigenvalues λ of the dynamic matrix are $\lambda_1=(r-\delta)$ and $\lambda_2=-r'$. Assuming that $r>\delta$, this equilibrium point is a saddle point (implying that the equilibrium is unstable); nevertheless, it becomes a stable focus when $r<\delta$. In fact, as demonstrated in the next section, it becomes the sole attractor in the ecological system and ensuring that M becomes extinct.

(b) The next equilibrium point of Eqs. (1) and (2) corresponds to an ecological system devoid of humans; that is, $M=K_M$ and $H=0$. Assuming that $M=K_M+\eta$ and $H=\varepsilon$, the matrix equation in the linear stability analysis becomes

$$\frac{d}{dt}\begin{pmatrix}\eta \\ \varepsilon\end{pmatrix} = \begin{pmatrix} -r & \left[rK_M D'(0) - \delta K_M/K_H\right] \\ 0 & r'\end{pmatrix}\begin{pmatrix}\eta \\ \varepsilon\end{pmatrix}. \tag{6}$$

Because the eigenvalues of the dynamic matrix are $\lambda_1=-r$ and $\lambda_2=r'$, this equilibrium point is also a saddle point (and therefore unstable).

(c) The point $H=0, M=0$ is unstable because Allee effect (Gonzales, 2011; Murray, 2004) is not assumed in our analysis. It corresponds to a demographic effect with a minimal critical population size, or density, to maintain species without collapse.

4. Equilibrium points outside axes: extinction threshold

Besides the three equilibrium points discussed in Section 3, specific forms of the generic functions $D(H)$ and $G(M)$ yield a set of points in the phase-space defined by $H>0$ and $M>0$. A rigorous investigation of these points usually requires additional information on these regular functions. Nevertheless, for our purposes, it is sufficient to specify the condition for non-existence of equilibrium points in this case. For numerical calculations, and better flow, we

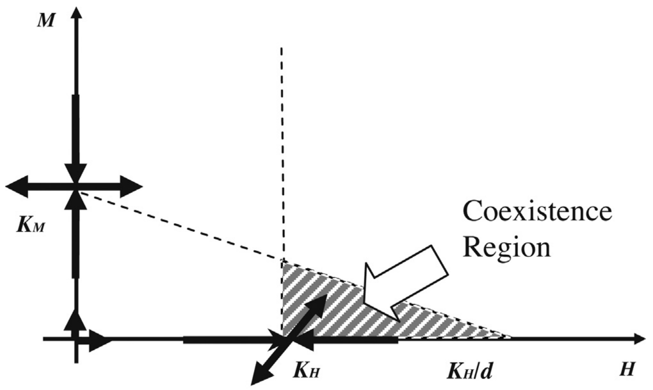

Fig. 1. Equilibrium points of the simultaneous prey–predator Eqs. (1) and (2). Three equilibrium points appear on the axes and coexistence is possible in the grey region. On the human H-axis, the equilibrium point $H = K_H$ (shown as unstable in the figure) becomes a stable focus under the extinction condition for the dimensionless depredation parameter $d = (\delta/r) > 1$ (Eq. (9), extinction threshold). Indeed, in this case, this stable focus is the only attractor in the dynamic system and megafauna extinction is inevitable. Furthermore, the grey triangle (potential region of coexistence) vanishes when $d = (\delta/r) > 1$.

define the dimensionless parameter $d = \delta/r$. In fact, in this paper, figures are referred to this dimensionless parameter.

In the dynamics of Eqs. (1) and (2), the coexistence equilibrium points (H_e, M_e) (see Appendix A) are the solutions to the pair of equations

$$\left(1-\frac{M_e}{K_M D(H_e)}\right)=\frac{\delta}{rK_H}H_e \quad \textit{and} \quad K_H G(M_e)=H_e. \tag{7}$$

Furthermore, given the conditions Eq. (4) we can write the basic inequalities:

$$0 \le \frac{M_e}{K_M} \le \left(1-\frac{\delta}{rK_H}H_e\right) \quad \text{and} \quad H_e \ge K_H, \tag{8}$$

which define the ultimate coexistence region (a triangle in the phase space geometry). Note that under the special condition $\delta < 0$, the above inequalities are reinforced and can be directly inferred to favor the development of M.

In Fig. 1, the triangulated grey area corresponds to the region of existence of these (eventual) equilibrium points when the inequalities (8) hold. The above-discussed three equilibrium points (Section 3) are also plotted in the figure for the case $r > \delta$. Importantly, when

$$\delta > r \quad \text{(extinction threshold)} \tag{9}$$

the basic inequalities (8) cannot be verified and no equilibrium points exist outside the axes (i.e. the grey region disappears in Fig. 1). Or explicitly, the upper bound for the first inequality in Eq. (8) will become negative when both the second inequality and (9) hold. In this case, as mentioned in Section 3, the point ($H = K_H$, $M = 0$) becomes a stable focus and the sole attractor in the system, meaning that species M is completely decimated. An algebraic approach to megafaunal (age-discriminated) extinction thresholds has also been implemented by Zuo et al. (2013) and Charnov and Zuo (2011). In our case, however, this threshold arises from the nonlinear dynamics Eqs. (1) and (2).

Note that Kiltie (1984) reported that seasonality (climactic fluctuations) raise the extinction of large species by decreasing their birth rate. In other words, climatic fluctuations could eventually enforce inequality (9) by decreasing r.

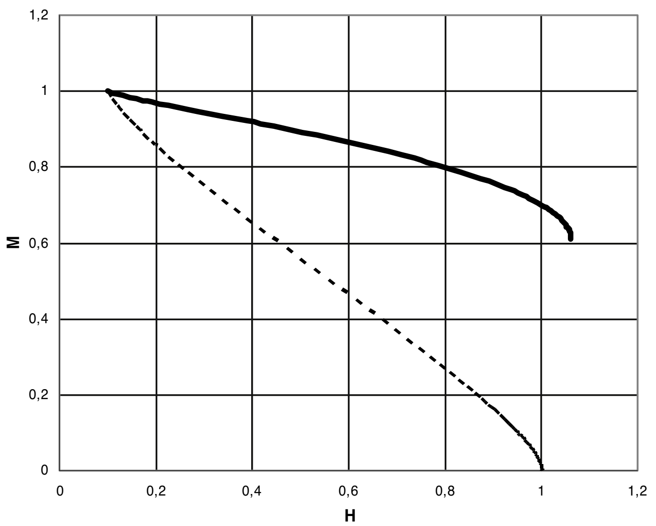

Fig. 2. Two typical trajectories on the phase space (M vs. H) when the extinction condition (9) is satisfied or not satisfied. Both trajectories begin at $H/K_H = 0.1$ and $M/K_M = 1$. The extinction case leads to $H/K_H = 1$ and $M = 0$, whereas the coexistence trajectory reaches an intermediate point (as discussed in Sections 3 and 4).

Condition (9) is ecologically plausible, because it states that extinction inevitably occurs when the depredation rate exceeds the species growth-rate. In the critical region we have $\delta = r$ and coexistence, eventually, emerges when $\delta < r$. Briefly, the extinction condition (9) could occur via the routes:

(i) Large depredation rate.
(ii) Slow growth rate, induced by climatic changes or some other factor.
(iii) Multifaceted interaction between depredation and altered growth rate (Gibbons, 2004).

Fig. 2 shows two typical numerical trajectories of M and H as functions of time in the phase-space. In one case, the condition (9) is imposed. Both trajectories begin at $H/K_H = 0.1$ and $M/K_M = 1$ (full carrying capacity). In the extinction case, the end-point is the stable focus $H/K_H = 1$ and $M = 0$. In the coexistence case, the trajectory terminates at an intermediate equilibrium point.

Fig. 3 plots the equilibrium solutions H_e and M_e as functions of the dimensionless depredation parameter $d = \delta/r$ for a

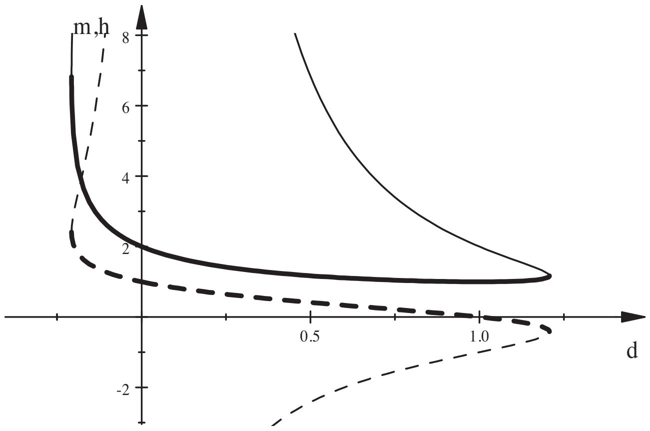

Fig. 3. Typical equilibrium solutions (Appendix A) of Eqs. (1) and (2) (explicitly Eq. (7)) with the choice simple $D(H) = 1$ and $G(M) = 1 + (M/K_M)^2$, as functions of the dimensionless parameter $d = (\delta/r)$. The solid lines correspond to the normalized number of modern humans $h = H_e/K_H$ and the dashed to the normalized megafauna $m = M_e/K_m$. Note that m (or M_e) becomes negative for $d > 1$, implying megafauna extinction. The positive dashed solutions when $d < 0$ indicate that species M may benefit of H and persist in this case. The four solutions (two-dashed and two-solid, which match) are distinguished by different thicknesses.

representative numerical case with $D(H) = 1$ and $G(M) = 1 + (M/K_M)^2$. As expected, no equilibrium solutions exist when the inequality (9) is satisfied ($d > 1$). Equilibrium solutions do exist when $d < 0$ (or $\delta < 0$), indicating that particular scenarios will benefit species M and ensure its survival. In this particular case for D and G, Eqs. (7) admits four solutions. These are superposed in Fig. 3 and discriminated by different thickness (see legend for clarity).

5. Extinction time and diffusion time: overkill hypothesis

The extinction time in the Late Pleistocene can be determined from the Lyapunov exponent (Prigogine, 1984). In principle, it can be obtained by simultaneously solving Eqs. (1) and (2). Numerically, the solutions require an infinite amount of time to reach their corresponding attractors. For practical purposes, however, we can linearize the equations around the extinction point (Section 3) and thereby upper-bound the elapsed extinction time τ_{ext} by (Appendix B)

$$\tau_{ext} \geq \frac{1}{\delta - r} \quad \text{with} \quad \delta > r. \tag{10}$$

Additional information on τ_{ext}, can be obtained from the spread of modern humans and their corresponding invasion of different habitats. Bénichou et al. (2011) established that intermittence (diffusion/relocation) is an optimal process of resource searching. A similar concept, intensive and extensive searching, has been discussed by Bartón and Hovestadt (2013) and Flores (2013). In this context, niche exploitation is modeled by slow diffusion motion (Appendix C), characterized by the diffusion coefficient D_f. For example, the diffusion coefficient for the invasion of Europe by modern humans around 50,000 years ago has been estimated as $D_f \sim 1600$ [km^2/yr] (Flores, 2011). Although modern humans were resisted by Neanderthal groups throughout this invasion, we nonetheless assume that D_f is generically applicable and adopt it in the present work.

The overkill hypothesis (Martin, 1967, 1984; Mosimann and Martin, 1975) posits that megafauna was (essentially) extinct at the arrival time of modern humans (Gillespie, 2002), being already decimated by fire control as an efficient ecosystems management tool. In this hypothesis, the diffusion and extinction times are equivalent and, the time required to diffuse over distance $\sqrt{A}$ (where A is the effective area) is approximately $\tau_D \sim A/D_f$ (see Appendix C). The extinction time τ_{ext} ($\sim \tau_D$) is then related to the diffusion coefficient by

$$\tau_{ext} \sim \frac{A}{D_f} \quad \text{(overkill hypothesis)} \tag{11}$$

where A is the effective area of the devastated habitat. Thus, according to Eq. (11), large areas will only be conquered over long periods. Conversely, high diffusion permits a short extinction time. Note that Eq. (11) is valid only if Eq. (9) is verified. Combining Eqs. (10) and (11), the parameters in our model are related by

$$(\delta - r) \sim \frac{D_f}{A}. \tag{12}$$

Eq. (12) provides useful estimations of the ecological and anthropological parameters in the theoretical overkill extinction framework. A particularly useful quantity is the relative rate $R = 1/r\tau_{ext}$ between depredation and growth, which from Eq. (12) is given by

$$R = \frac{\delta - r}{r}. \tag{13}$$

This relationship is evaluated for different cases in the next section.

6. Rough estimation of megafaunal extinction time from ecological and archaeological data

Using the complementary expressions (10) and (11), we can evaluate the parameters in different ecosystems that were decimated by humans. We remark that these evaluations, and their consequent predictions, are coarsely estimates only (we assume $D_f \sim 1600$ [km^2/yr], Section 5).

Ecological growth rates are usually difficult to measure (Begon et al., 1996). In the event of massive extinctions, data collection is complicated by the large volume of lost information. For instance, the Late Pleistocene witnessed severe depletion of giant herbivores. For conceptual purposes, we adopt the African elephant (*Loxodonta africana*) as a representative megafaunal species. In fact, it is a well documented species allowing to make comparable calculations in our model (Section 5) and, ultimate, justified by the reasonable predictions for elapsed time in the three following cases (a, b and c). Even for this extant species, estimations are difficult because the parameters depend on captivity status (wild or captive), sex, and a variety of other factors. Therefore, we follow von Aarde et al. (1999), who documented the population growth of African elephants at Kruger National Park, where culling was banned from 1995. Over the next decade, the population grew from (approximately) 7300 to 9000. Thus, the *per capita* growth rate may be reasonably estimated as $r_{eleph} \sim 0.019$ [1/yr]. In comparison, for ancient modern humans, a growth rate of $r' \sim 0.01$ [1/yr] was assumed (Fort and Méndez, 1999). Moreover, von Aarde et al. (1999) also estimated the equilibrium density ρ_{elph} of the order of ∼0.37 elephants/km^2. Although these values may be regarded as purely hypothetical and derived under unrealistic conditions, they provide useful first-approach data for our coarse calculations. In every case, we assume that elephants at Kruger National Park are representative of the megafauna lost during the Late Pleistocene.

(a) *Australia*. The arrival of humans in Australia was accompanied by a shift toward dry climatological conditions. The total area of Australia 7.7×10^6 [km^2] can be assumed as the effective area in the Pleistocene epoch. From Eq. (11), the elapsed extinction time is then estimated as $\tau_{ext} \sim 4800$ [yrs]. Although the human colonization time has not been clarified, it is known to have occurred around 49,000 years BP and was widespread around 40,000 years BP (David, 1997; Rule, 2012). Therefore, our coarse estimate is consistent with archaeological dates and may be reasonably assumed as the elapsed extinction time in this case. The relative rate (13) is then estimated as $R \sim 0.01$ and the depredation parameter becomes $\delta \sim 0.0192$ [1/yr].

(b) *North America*. According to Gill et al. (2009), megafauna in North America became extinct around 14,800–13,700 years ago, and were likely decimated by human impact. To conceptualize these dates, we emphasize that ancient America was occupied, for instance, at Monte Verde (Chile) around 14,600 years ago (Fiedel, 2002) and Buttermilk Creek (possibly) 15,500 years ago (Walters et al., 2011; Goebel et al., 2008). The geographical surface area of Canada and the United States is approximately 10×10^6 [km^2] and 9.6×10^6 [km^2], respectively. Although not all regions are hospitable to life, World Bank data report that 6.9% and 45% of the area covered by Canada and the United States, respectively, is agriculturally cultivable. Assuming these area as a first coarse estimate of viable life coverage, the effective livable region of the North Americas is $A \sim 5 \times 10^6$ [km^2]. In this case, Eq. (11) gives the estimated elapsed extinction time as $\tau_{ext} \sim 3000$ [yrs]. The relative rate is calculated as $R \sim 0.018$ and the depredation parameter $\delta \sim 0.0193$ [1/yr].

(c) *Africa critical case*. Anatomically modern humans purportedly evolved approximately 200,000 years ago in Africa (McDougall et al., 2005; Fagan, 2012), where they have coexisted with numerous extant megafauna. Nevertheless, there are strong indications of continued extinction on the African continent. For example, according to the International Union for Conservation of Nature, the *Western Black Rhino* is officially extinct. This slow process of large-scale decimation in Africa represents a critical case ($\delta \sim r$, Appendix B), in which an eigenvalue of the dynamic matrix (5) is zero, and a decreasing temporal power law behavior is expected. Setting $H = K_H$, $\delta = r$ and (for simplicity) $G(M) = 1$ in Eqs. (1) and (2), the evolution equation for M is easily solved to give the following power law equation:

$$\frac{1}{M} = \frac{1}{M_o} + \frac{rt}{K_M D(K_H)}, \tag{14}$$

where $M_o \gg 1$ is the initial condition. In this slow (non-exponential) regimen, the *critical time* τ_c can be roughly estimated by setting $M_{final} = 2$ (two individuals, a technical requirement for extinction) in Eq. (14). The analytical expression of the critical time is

$$\tau_c \sim \frac{K_M D(K_H)}{2r}. \tag{15}$$

To evaluate τ_c, we must estimate the growth decreasing factor $D(H)$ imposed by territory usurpation of Kruger. First, note that τ_c does not explicitly depend on the effective area. In fact, if the inhabitable area is restricted to ΔA, we can set $D = \Delta A/A$ and because $K_M = \rho A$, the critical time simplifies to $\tau_c \sim \rho \Delta A/2r$. At Kruger National Park, elephants are confined within $\Delta A = 19,000\,\text{km}^2$. Assuming a population density of $\rho \sim 0.37\,[1/\text{km}^2]$ (von Aarde et al., 1999), the critical time is given by $\tau_c \sim (19,000 \times 0.37)/(0.019 \times 2) \sim 185,000$ [yrs], roughly consistent with the mentioned emergent-time of anatomically modern humans in Africa.

7. Allometric considerations: extinction body-mass threshold

Following the pioneering work of Huxley (1932) several decades ago, allometry has become universally applied to biological and ecological systems. Biological allometry considers differences between a same parameter (for instance, rates) defined through a mathematical power law (exponents different of unit) in terms of a biological quantity as for instance body-mass. In particular, parameters such as reproductive rates, generation times, and physiological rates are fundamental to modeling population growth and dynamics. Allometry has also been envisaged as valid in massive extinction modeling (Brook and Wand Bowman, 2005; Peters, 1983; Zuo et al., 2013; Charnov and Zuo, 2011). Furthermore, for any given species, the population growth rate is related to the individual-averaged mass W as $r = \alpha/W^{\nu}$ with α proportionality constant. The exponent $\nu \sim 0.25$ appears to fit most biological species (Günther and Morgado, 2004; Brook and Wand Bowman, 2005). Assuming that depredation is a mass selective process, we can assume the following functional form of the interaction parameter in Eq. (1): $\delta = \beta W^{\nu'}$ (with $\nu' > 0$), where the massless parameter β depends on the various biological and cultural factors as mentioned in Section 1 (such as δ). Consequently, the extinction condition, in terms of the body mass threshold Eq. (9), becomes

$$W^{\nu+\nu'} > \alpha/\beta \tag{16}$$

This suggests that species with averaged body mass below the threshold $W_c = (\alpha/\beta)^{1/(\nu+\nu')}$ will escape extinction by depredation (Koch, 2006). Similar conclusions on harvesting and adult mortality were obtained by Zuo et al. (2013). Note that Sibly and Brown (2007) conducted an evolutionary data analysis incorporating ecology and phylogeny (as a second axis). Allometric considerations and their consequences are thoroughly discussed in Fagan et al. (2010) and references therein.

8. Conclusions and open questions

Using a large-scale model Eqs. (1) and (2), we established an extinction threshold for megafaunal decimation during the Late Pleistocene. From the model, we also estimated the elapsed extinction times following human colonization of individual continents.

The estimated quantities are roughly consistent with archaeological records. The threshold extinction condition was given as a direct relationship between the depredation and growth rates (see Eq. (9)). Allometric considerations allow the resetting of this condition as a mass threshold (Section 7). Furthermore, assuming that the overkill hypothesis Eq. (11) is applicable to the Late Pleistocene, we evaluated coarsely the elapsed time of two major large-scale prehistoric extinction events; namely, the decimation of terrestrial megafauna in Australia (4800 years) and North America (3000 years). On the other hand, Africa, where representative megafauna are extant, was presented as a critical case with a power-law decline in population. In this case, the critical time roughly coincides with the emergence of anatomically modern humans some 200,000 years BP in Africa. We have used, as representative actual megafauna, elephants in Kruger Park. This is justified because they are a well documented species and, finally, our results validate this assumption.

Globally, large-scale megafaunal life persists in oceans. Whales, like elephants, are representative of constant decimation and can be used as a prototype species to realize rough parameter estimates. Megafaunal extinction can be traced to the beginnings of modern humans around 50,000 years BP and no evidence suggests that it will terminate nowadays. The disastrous ecological consequences of human colonization, such as occurred at Easter Island around 1400 AD (Diamond, 2005; Bologna and Flores, 2008), appear to be a sadly natural part of our evolution.

Acknowledgements

This work was supported by FONDECYT 1120344. Valuable discussions were carried-out with H. Cortes (ULS), M. Bologna (UTA) and K. Chandia (UTA).

Appendix A.

The linearization technique used in Section 3 is a standard tool for nonlinear systems (Boccara, 2010; Murray, 2004; Lakshmanan and Rajasekar, 2002). Briefly, assume the nonlinear functions $F_1(H, M)$ and $F_2(H, M)$ and the coupled evolution equations (for instance (1) and (2)):

$$\begin{aligned} \frac{dH}{dt} &= F_1(H, M), \\ \frac{dM}{dt} &= F_2(H, M), \end{aligned} \tag{17}$$

with an equilibrium point (H_e, M_e) where

$$F_1(H_e, M_e) = F_2(H_e, M_e) = 0. \tag{18}$$

Stability criterion becomes from the study of the evolution around of this equilibrium point. Namely, the evolution equations for the (small) perturbations $\eta = M - M_e$ and $\varepsilon = H - H_e$. From the pair (17), one obtains formally the linearized evolution equations (derivatives evaluated in the equilibrium point):

$$\frac{d}{dt}\begin{pmatrix} \varepsilon \\ \eta \end{pmatrix} = \begin{pmatrix} \partial F_1/\partial H & \partial F_1/\partial M \\ \partial F_2/\partial H & \partial F_2/\partial H \end{pmatrix} \begin{pmatrix} \varepsilon \\ \eta \end{pmatrix} \tag{19}$$

The eigenvalues λ_1 and λ_2 of the above matrix (see for instance (5) and (6)) determine the stability criterion. For instance, if both eigenvalues are positive then it becomes an unstable equilibrium point, and so on (see Murray (2004) for classifications of equilibrium points).

Appendix B.

The inverse of the eigenvalues (real part) of the dynamic matrix (19), $1/\lambda_1$ and $1/\lambda_2$ are related to characteristic times for exponentially fall (or depart) in the corresponding equilibrium point. In the case of Section 5, to consider extinction (Eq. (10)), both eigenvalues are negatives when $\delta > r$. It describes the (only) attractor of the prey–predator model Eqs. (1) and (2) and related to the extinction condition (9). In the critical case where $\delta = r$ (Africa case, Section 6) one eigenvalue becomes zero and it is expected an algebraic behavior like (14).

Appendix C.

In the work was used a coefficient of diffusion D_f which makes reference to the well-known differential equation (Boccara, 2010; Murray, 2004)

$$\frac{\partial n}{\partial t} = D_f \nabla^2 n, \qquad (20)$$

corresponding to a slow type of spatial motion for the scalar density n. The characteristic size x, of the dispersing cloud, varies as $x^2 \sim D_f t$ and is related, in our case, to niche exploitation. We assume $x^2 \sim A$ (effective area) in Section 5. The diffusion–relocation process, mentioned in the paper (also, Section 5), is linked to a diffusive and ballistic ($x \sim t$) superposition, a limit case of the paper by Bénichou et al. (2011) and also discussed in Flores (2013).

References

Alroy, J., 2001. A multispecies overkill simulation of the end-Pleistocene megafaunal mass extinction. Science 292, 1893–1896.

Bartón, K.A., Hovestadt, T., 2013. Prey density, value, and spatial distribution affect the efficiency of area-concentrate search. J. Theor. Biol. 316, 61–69.

Begon, M., Harper, J.L., Townsend, C.R., 1996. Ecology. Blackwell Science, London.

Belovsky, G.E., 1988. An optimal foraging-based model of hunter–gatherer population dynamics. J. Anthropol. Archaeol. 7, 329–372.

Bénichou, O., Loverdo, C., Moreau, M., Voituriez, R., 2011. Intermittent search strategies. Rev. Mod. Phys. 83, 81–113.

Boccara, N., 2010. Modeling Complex Systems, 2nd ed. Springer, Berlin.

Bologna, M., Flores, J.C., 2008. A simple mathematical model of society collapse applied to Eastern Island. Europhys. Lett. 81, 48006.

Brook, B., Wand Bowman, D.M.J.S., 2005. One equation fits overkill: why allometry underpins both prehistoric and modern body sized-biased extinctions. Popul. Ecol. 47, 137–141.

Brown, K.S., et al., 2009. Fire as an engineering tool of early modern humans. Science 325, 859–862.

Callegari, S., et al., 2013. An agent-based model of human dispersals at a global scale. Adv. Complex Syst. 16, 1350023.

Charnov, E.L., Zuo, W., 2011. Human hunting mortality threshold rules for extinction in mammals (and fish). Evol. Ecol. Res. 13, 431–437.

Daniau, A.-L., d'Errico, F., Sanchez Goñi, M.F., 2010. Testing the hypothesis of fire use for ecosystem management by Neanderthal and upper paleolithic modern human populations. PLoS ONE 5, e9157.

David, B., et al., 1997. New optical and radiocarbon dates from Ngarrabullgan Cave, a Pleistocene archaeological site in Australia: implications for the comparability of time clocks and for the human colonization of Australia. Antiquity 71, 183–188.

Diamond, J., 2005. How Societies Choose to Fail or Succeed. Penguin Books, London, England.

Elmhagen, B., Angerbjörn, A., 2001. The applicability of metapopulation theory to large mammals. Oikos 94, 89–100.

Fagan, W.F., Lynch, H.J., Noon, B.R., 2010. Pitfalls and challenges of estimating population growth rate from empirical data: consequences for allometric scaling relations. Oikos 119, 455–464.

Fagan, B.M., 2012. Archaeology: A Brief Introduction. Person Press, London.

Fiedel, S.J., 2002. Initial human colonization of the Americas: an overview of the issues and the evidences. Radiocarbon 44, 407–436.

Flores, J.C., 2011. Diffusion coefficient of modern humans out competing Neanderthals. J. Theor. Biol. 280, 189–190.

Flores, J.C., 2013. Intermittence for humans spreading 45,000 years ago: from Eurasia to the Americas. Hum. Biol. 85, 789–796.

Fort, J., Méndez, V., 1999. Time-delay theory of the Neolithic transition in Europe. Phys. Rev. Lett. 82, 867–869.

Foster, M.A., 2003. Self-organised instability and megafaunal extinctions in Australia. Oikos 103, 235–239.

Gibbons, R., 2004. Examining the Extinction of the Pleistocene Megafauna (http://www.stanford.edu/group/journal/cgi-bin/wordpress/wp-content/uploads/2012/09/Gibbons_NatSci_2004.pdf).

Gill, J.L., et al., 2009. Pleistocene megafaunal collapse, novel plant communities, and enhanced fire regimes in North America. Science 20, 1100–1103.

Gillespie, R., 2002. Dating the first Australians. Radiocarbon 44, 455–472.

Goebel, T., Walters, M.R., O'Rouke, D.H., 2008. The Late Pleistocene dispersal of modern humans in the Americas. Science 319, 1497–1502.

Gonzales, E., et al., 2011. Dynamical complexities in the Leslie–Gower predator–prey model as consequences of the Allee effect on prey. Appl. Math. Model. 35, 366–387 (Also (2012) 36, 860–862).

Günther, R., Morgado, E., 2004. Time in physics and biology. Biol. Res. 37 (4 Suppl. A), 759–765.

Hamilton, M.J., Buchanan, B., 2007. Spatial gradients in Clovis-age radiocarbon dates across North America suggest rapid colonization from the north. PNAS 104, 15625–15630.

Hortola, P., Martinez-Navarro, B., 2013. The quaternary megafaunal extinction and the fate of Neanderthals: an integrative hypothesis. Quat. Int. 295, 69–72.

Huxley, J.S., 1932. Problems of Relative Growth. Methuen, London.

Kiltie, R.A., 1984. Seasonality, gestation time and large mammal extinctions. In: Martin, P.S., Klein, R.G. (Eds.), Quaternary Extinction: A Prehistoric Revolution. University of Arizona Press, Tucson, pp. 299–314.

Koch, P.L., et al., 2006. Late quaternary extinctions: state of the debate. Annu. Rev. Ecol. Evol. Syst. 37, 215–250.

Lakshmanan, M., Rajasekar, S., 2002. Nonlinear Dynamics, Integrability, Chaos and Patterns. Springer, Berlin.

Le Bellac, M., 1992. Quantum and Statistical Field Theory. Oxford Sciences Publications, England.

Leslie, P.H., 1948. Some further notes on the use of matrices in population mathematics. Biometrika 35, 213–245.

Martin, P.S., 1967. In: Martin, P.S., Wright, H.E. (Eds.), Pleistocene Extinctions: The Search of a Cause. Yale University, New Haven.

Martin, P.S., 1984. Prehistoric overkill: the global model. In: Martin, P.S., Klein, R.G. (Eds.), Quaternary Extinctions: A Prehistoric Revolution. University of Arizona Press, pp. 354–403.

McBrearty, S., Brooks, A.S., 2000. The revolution that wasn't: a new interpretation of the origin of modern human behavior. J. Hum. Evol. 39, 452–563.

McDougall, I., Brown, F.H., Fleagle, J.G., 2005. Stratigraphic placement and age of modern humans from Kibish, Ethiopia. Nature 433, 733–736.

Mithen, S., 1993. Simulating mammoth hunting and extinction: implications for the late Pleistocene of the central Russian Plain. Archeol. Pap. Am. Anthropol. Assoc. 4, 163–178.

Montoya, D., Alburquerque, F.S., Rueda, M., Rodríguez, M.A., 2010. Species' response patterns to habitat fragmentation: do trees support the extinction threshold hypothesis? Oikos 119, 1335–1343.

Mosimann, J.E., Martin, P.S., 1975. Simulating overkill by Paleoindians. Am. Sci. 63, 304–313.

Murray, J.D., 2004. Mathematical Biology, vols. I and II., 3rd ed. Springer, Berlin.

Peters, R.H., 1983. The Ecological Implications of Body Size. Cambridge University Press, New York.

Prigogine, I., 1984. From being to becoming: time and complexity in the physical sciences. University of Chicago Press, Chicago.

Rule, S., et al., 2012. The aftermath of megafaunal extinction: ecosystem transformation in Pleistocene Australia. Science 23, 1483–1486.

Saether, B.-E., Bakke, O., 2000. Avian life history variation and contribution of demographic traits to the population growth rate. Ecology 81, 642–653.

Sibly, R.M., Brown, J.H., 2007. Effect on body size and lifestyle on evolution of mammal life histories. PNAS 104, 17707–17712.

Troyer, E.M., Cameron, S.E., Sunquist, M.E., Goswami, V.B., Oli, M.K., 2014. Density dependence or climatic variation? Factors influencing survival, recruitment, and population growth rate of Virginia opossums. J. Mammal. 95, 421–430.

von Aarde, R., Whyte, I., Primm, S., 1999. Culling and the dynamics of the Kruger National Park African elephant population. Anim. Conserv. 2, 287–294.

Walters, M.R., et al., 2011. The Buttermilk Creek Complex and the origin of Clovis at the Debra L. Friedkin site, Texas. Science 331, 1599–1603.

Whittington, S.L., Dyke, B., 1984. Simulating overkill: experiments with the Mosimann and Martin model. In: Martin, P.S., Klein, R.G. (Eds.), Quaternary Extinctions: A Prehistoric Revolution. University Arizona Press, Tucson, pp. 451–465.

Zuo, W., Smith, F.A., Charnov, E.L., 2013. A life-history approach to the Late Pleistocene megafaunal extinction. Am. Nat. 182, 524–531.